International Journal of Steel Structures 15(3): 623-632 (2014)
DOI 10.1007/s13296-015-9009-3
ISSN 1598-2351 (Print)
ISSN 2093-6311 (Online)

International Journal of
STEEL
STRUCTURES
www.springer.com/journal/13296

Distortion Induced Fatigue of Deck Plate at Rib Intersection with Diaphragm in Orthotropic Steel Deck

Rong Liu[1], Bo Wang[2], and Yuqing Liu[3,*]

[1]*College of Civil and Transportation Engineering, Hohai University, Nanjing 210098, China*
[2]*Department of Bridge Engineering, Tongji University, Shanghai 200092, China*
[3]*Department of Bridge Engineering, Tongji University, Shanghai 200092, China*

Abstract

Toe-deck (TD) fatigue due to wheel induced distortion of orthotropic steel decks (OSDs) was reported by laboratory tests. The existing OSDs could probably suffer the TD fatigue and is evaluated using the hot spot stress (HSS) method. The wheel induced stresses of the trough-deck welded joint are analyzed using the shell model. The influences of HSS with mesh size, stress extrapolation, element shape function and the hot spot location variation are checked. TD fatigue durability using the monitored traffic data and the design specifications are discussed. Results demonstrate that the weld toe of the joint suffers wheel induced stress concentration and frequent stress cycles. The refined shell model using the 4-node-shell elements results in nearly constant HSS. TD fatigue durability of the 12mm deck with 50mm asphalt pavement falls below the designed service life that might explain the observed fatigue cracks in the vicinity of the deck toe by laboratory tests and the in-site observation. The TD fatigue evaluation using the HSS method may be utilized to get a conservative OSD design.

Keywords: orthotropic steel decks, fatigue, durability, hot spot stress, FEA

1. Introduction

Orthotropic steel decks (OSDs) with closed ribs (trough ribs) are used in beams and cable-supported bridges owing to the lighter self-weight, the higher load carrying capacity and the faster fabrication speed. The fatigue damages of OSDs under the wheel loads are present in several countries (Wolchuk, 1999; De Jong, 2004; Miki 2006). Most OSDs in China were designed with little geometric variation and without the detailed fatigue assessment. However, the fatigue cracks were reported in two major suspension bridges after about 10 years' service. The fatigue damages reported in Humen Bridge (Zhou, 2010; Pan *et al*., 2011) and Jiangyin Bridge (Zhang *et al*., 2013) make the fatigue study of OSDs an urgent issue in China since the owners worried about the durability of other OSDs in service and those under construction. It is necessary to reevaluate the fatigue with the appropriate methods to figure out the causes.

Received November 9, 2014; accepted May 3, 2015;
published online September 30, 2015

*Corresponding author
Tel: +86-21-65983116, Fax: +86-21-65986507
E-mail: yql@tongji.edu.cn

The fatigue cracks of the deck plate at the rib intersection with the diaphragm were usually regarded as the root-deck crack and the weld throat crack (Miki *et al*., 1995; JAR, 2002), as shown in Fig. 1(a). The root-deck fatigue was studied in several researches (Xiao *et al*., 2008; Ya *et al*., 2011). However, the full scale tests conducted by Sim *et al*. (2009) revealed that the toe-deck cracks appeared in 5 specimens with weld melt through while the root-deck crack appeared in 1 specimen. The study concluded that based on the fixed loading pattern, the trough-deck welds are more vulnerable to the cracks initiating from the weld toe, not the weld root. Full scale tests by Mori *et al*. (2006) showed that toe-deck crack might occur in the joint with 75% weld penetration. The small size tests by Zhao (2010) showed that the 15 specimens under the trough loaded deck plate bending came to the toe-deck failure. The small size tests conducted by Yuan (2011) confirmed that the toe-deck crack appeared in 48 specimens of the total 100 specimens. It seems that the possibility that the toe-deck fatigue damage might occur in the trough-deck joint should not be eliminated. In Jiangyin Bridge and Humen Bridge, the open snip of a quarter-aperture with 35mm radius is used in the diaphragm at the junctions of the trough with the deck plate. The weld toe might suffer the toe-deck fatigue damage, as shown in Fig. 1(b).

Limited research of the toe-deck fatigue in the vicinity

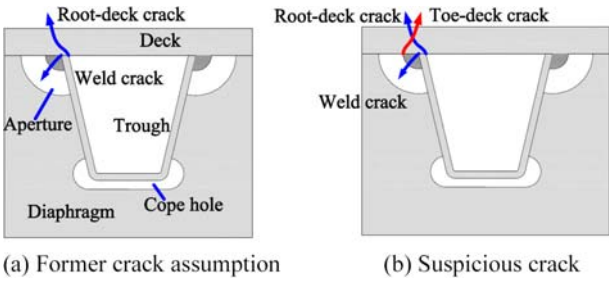

Figure 1. Fatigue cracks of trough-deck welded joint.

of the aperture has been carried out to evaluate the fatigue. The aperture is not suggested by AASHTO (2004) and CEN (2006). Some researches regarding the fatigue of the deck plate at the rib intersection with the floor beam or the diaphragm discussed the possible fatigue of the root-deck fatigue (Wolchuck, 1999; Kolstein, 2007; Fisher and Roy, 2014). Most of the tests with the toe-deck fatigue did not include the diaphragms' constrains. This paper focuses on the toe-deck fatigue within the quarter-aperture of the diaphragm.

The nominal stress method for fatigue evaluation is dominant in the steel bridge fatigue design specifications (CEN, 2006; AASHTO, 2004; JAR, 2002). However, the strength of the joint is not the subject in Europe and USA (United States of America) since the detail with aperture is not a standard use. The nominal stress and the corresponding strength are difficult to evaluate the complex OSDs. The hot spot stress (HSS) method comes to be used in the pipe welded joints of ships and offshore structures in recent years (Hobbacher, 2009). The HSS of a welded joint owing to the structural geometry and the applied loads are included in the stress analyzing model while the notch effect and the defects due to welding are determined by the fatigue tests of the welded joint. Compared with the nominal stress method, the HSS definition and the analysis models seem to be more explicit and operable for the complex details of OSDs (Liu *et al*., 2014a,b).

In this paper, the HSS method is used to evaluate the toe-deck fatigue of the joint. Depending on AASHTO, the features of topology that may affect the accuracy of the analytical solution should be checked. The element shape function, the mesh size, the stress extrapolation equation and the hot spot approximation of the shell model that might affect the accuracy of HSS are checked in this paper. The cause of the toe-deck fatigue is analyzed according to the mechanical behavior of the joint subjected to wheel loads. The fatigue damage accumulation is evaluated to check whether the fatigue sample contradicts with the HSS theory or the original design is not conservative.

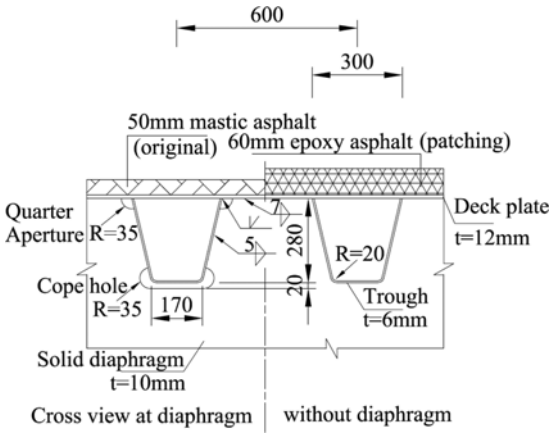

Figure 2. Structural details of orthotropic steel deck (Unit: mm)

2. Finite Element Models

2.1. Structural details of OSD

OSD consists of a deck plate stiffened with longitudinal troughs and it is supported on the diaphragms. The OSD and the asphalt pavement on the top surface of the deck plate constitute the bridge deck system carrying the truck loads. The OSDs with 12 mm thickness deck plates and 6 mm thick troughs are mainly used in the suspension bridges built in the early 1990's in China. The typical cross section is showed in Fig. 2. For Jiangyin Bridge, the original 50 mm thick mastic asphalt pavement was damaged less than 3 years after service. 60 mm epoxy asphalt was used to replace the original one. However, the new pavement was not strong enough and it required frequent patching.

At the diaphragm section, the deck plate and the troughs are connected with a longitudinal partial-penetrated-groove weld with 75% penetration. The deck plate and the diaphragm are connected with a transverse fillet weld of 7 mm weld leg. The trough webs and the diaphragm are connected with a vertical fillet weld of 5 mm weld leg. The quarter-aperture of 35 mm radius is used in the diaphragm to make each weld a continuous one without interruption during welding. The continuous welds are intended to have fewer defects and the interactions between the welds are regarded to be reduced using the aperture.

2.2. Building of shell models

The shell model of OSD in the shoulder lane with heavy traffic flow is built. The model comprises of 5 diaphragms and 7 troughs. The length of the model is 12.8 m and the width is 4.2 m. The diaphragm depth is 1m and the diaphragm interval is 3.2 m. Since most of the trucks are distributed in the shoulder lane, the trough

under the wheel near the mid-lane of the truck driving on the shoulder lane is taken as the target trough. The geometric data follow the design parameters of Humen Bridge and Jiangyin Bridge where the OSD fatigue cracks were reported. The details of OSD are shown in Fig. 2.The deck plate thickness is 12 mm and the trough rib is 6 mm and the diaphragm is 10 mm. The aperture radius is 35 mm.

The FEA software ANSYS is used to analyze the deck model (Ansys Inc., 2013). Two kinds of shell elements are used. That is shell181 with 4 nodes and linear shape function and shell281 with 8 nodes and non-linear shape function. Each node has 6 degrees of freedom. That is the translations in the nodal x, y, and z directions and rotations about the nodal x, y, and z-axes. The deformation shape functions of shell281 are quadratic in both in-plane and out-plane directions. The linear elastic material properties of structural steel are assigned to the FE model. Young's modulus is 206GPa and Poisson's ratio is 0.3.

The shell model is presented in Fig. 3. The fillet weld geometries are simplified as the elements of the deck plate and the trough ribs having the same edges and nodes. The nodes on the edges of the diaphragm are fixed in all directions and the nodes along the edges of the deck plate and the troughs are pin supported. Most of the shapes of the shell elements are rectangular. The length and the width of the element are almost the same and the aspect ratio is close to 1.0. The element size of 3 mm by 3 mm in the vicinity of the trough-deck joint is used to check stresses near the joint.

Although the asphalt pavement has an influence on the stress of the deck plate (Ji and Liu, 2013), the pavement is regarded as the load dispersal effect with 45 degree spread angles through the pavement thickness. The reasons for eliminating the composite effects of the pavement in this paper are that the original 50 mm thick pavement over the 12 mm deck plate suffers severe crack and debonding damage. The composite effect of the pavement might overestimate the behavior of the pavement to deck interaction. The replaced 60 mm pavement seems to be improved according to laboratory tests and the first few years' field use. However, the local repair or replacement of the pavement is frequent. Everywhere distributed patches of the pavement and the bump of the driving truck seem to prove that the durability of the pavement over the thin deck plate is over optimistic. Thus, it is better to exclude the stress decrease effect of the pavement to get a conservative design of the thin deck plate.

The single wheel and double wheel loads are applied in the model. The unit load 1 kN is used for both the single and the double wheels. The wheel to pavement contact area is set as (600+50×2) mm × (200+50×2) mm for the double wheels and (300+50×2) mm×(200+50×2) mm for the single wheel.

3. Stress of Deck Plate Subjected to Wheel Load

3.1. Stress on bottom surface of deck plate

The unit 1 kN double wheel load is applied on the deck plate with the center coincident with the trough-deck intersection point. The deformation of the joint subjected to wheel load is shown in Fig. 4. The deck plate above the aperture carries bending moment M2 and the trough wall carries M3. The bending moments M2 and M3 balance the bending moment M1 that is carried by the deck plate within the trough and produced by the wheel load. Since the 6 mm trough wall is slender compared with the 12 mm deck plate, M2 is much larger than M3. The wheel load makes the deck plate above the aperture subjected to hog bending. Once the wheel stays away from the joint, the bending moment is released. The joint undergoes one major stress cycle and fatigue damage might occur given adequate stress cycles. Given the aperture

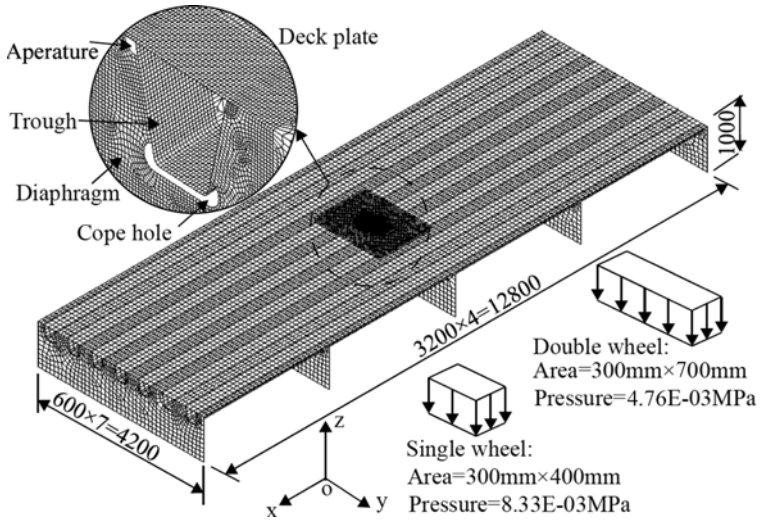

Figure 3. Finite element model of a steel bridge deck (Unit: mm).

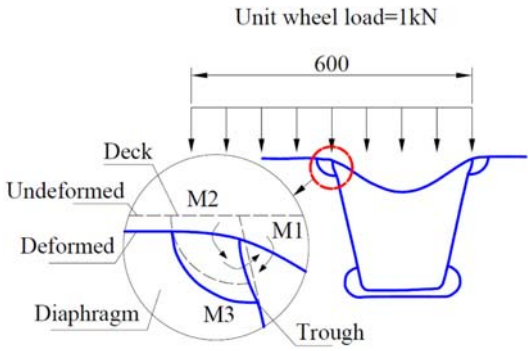

Figure 4. Deformation of the joint under double wheel load.

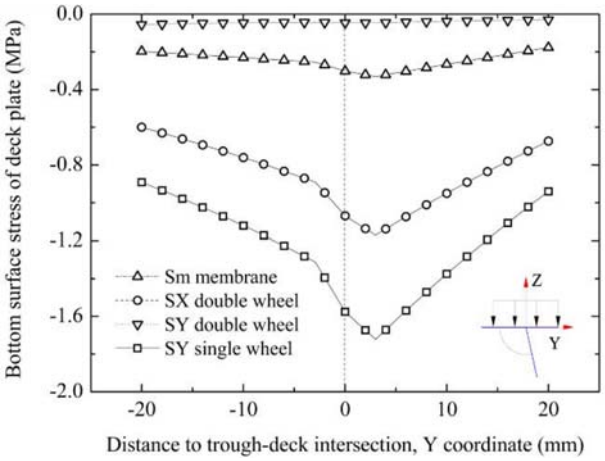

Figure 5. Stress distribution of deck plate in transverse direction.

is not cut from the diaphragm, the bending deformation of the deck plate and the trough wall is constrained by the diaphragm. It seems that the aperture weakens the diaphragm and makes the weld toe of the joint expose to stress cycles.

The stress at the bottom surface of the deck plate is shown in Fig. 5. M2 results in transverse compressive stress σ_y at the bottom surface of the deck plate above the aperture. However, the tensile residual stress of welding may overcome the compressive stress and the weld toe could possibly subject to net tensile stress that is adverse to fatigue resistance. The aperture makes the weld toe of the joint expose to high level stress concentration that is unfavorable for fatigue resistance.

The transverse bending stress σ_y is dominant compared with the longitudinal stress σ_x and the membrane stress σ_m. The fatigue evaluation of the joint uses the transverse stress component σ_y in this paper. Although several health monitoring systems have been built for bridges in China, most of them fail to identify or predict the steel deck fatigue failure according to the monitored strains of the deck. The stress distribution of the joint shown in Fig. 5 might explain the failure. The sensors for the steel deck health monitoring systems are typically located on the

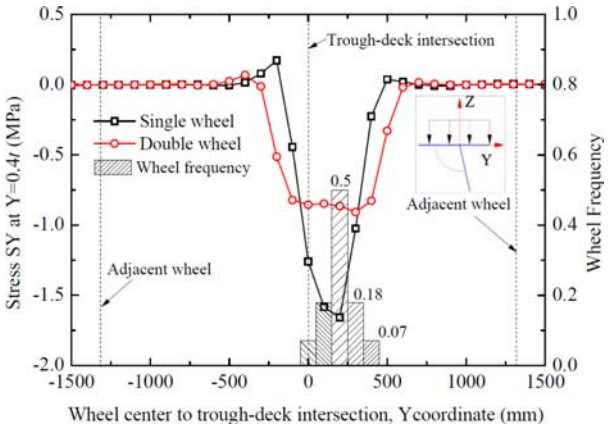

Figure 6. Stress under transversely located wheel load.

deck plate without diaphragm. The aperture of 35 mm radius is too small to set the long wire-vibration strain gauges or the fiber strain gauges that are used for long term monitoring. The deck inside the trough is isolated for strain monitoring. Thus, additional sensors should be set close to the deck plate within the aperture to capture the wheel induced strain peaks.

3.2. Stress under transverse located wheel load

The stress σ_y against wheel location variation in the Y direction is shown in Fig. 6. The largest stress appears once the double wheel load is transversely located directly above the trough wall to deck plate junction. It appears that the wheel path over the junction is the critical path that might cause the maximum stress range of the joint.

The transverse stress influence range of the joint in the *y* direction is less than 900 mm. The transverse influence range is small compared to the 1.3 m wheel distance between the truck under consideration and the truck driving on the adjacent lane. The fatigue contribution of the adjacent lane is omitted. The transverse influence range is small compared to the 1.8 m wheel distance of an axle. The wheel load except the axle load is used to get the stress range of the joint.

The stress σ_y decreases with the wheel deviating from the critical driving path. Given that all the trucks are supposed to drive on the critical path, it results in a moderate fatigue design of the joint. The assumption is used in bridge design practice in America (AASHTO, 2004). However, it might be reasonable to consider the frequency of wheel occurrence along the transverse direction, since the relaxed driving habit in China gives a larger deviation from the critical path. According to Eurocode (CEN, 2006), the wheel transverse occurrence range is 500mm with a normal frequency distribution. The stress decrease and the frequency of occurrence with wheel transverse location variation are included in this paper.

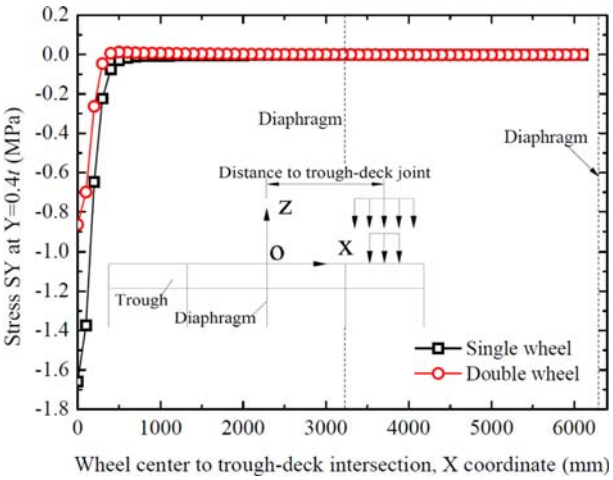

Figure 7. Stress under longitudinally located wheel load.

3.3. Stress under longitudinal moving wheel load

The stress σ_y against wheel location variation in the x direction is shown in Fig. 7. The stress influence line ranges about twice the deck span length. The length of the shell model is about 4 times of the deck span length between the adjacent diaphragms. It can suppress the influence of the boundary approximation.

The wheel that is placed over the diaphragm results in a major stress valley. Given the wheel passes away from the diaphragm, the stress of the joint decreases sharply. The wheel has negligible influence on the stress provided it is located about 1 m away from the diaphragm. It appears that the influence line of the joint is short compared with the 4.3 m axle distance of the fatigue truck specified by AASHTO (2004). Each time for one wheel load longitudinally driving over the joint, it causes three stress cycles. That is one major stress range from the valley to the peak and anther small range from the peak to zero. For a typical 4-axle truck, it causes four major stress cycles and the heavy traffic flow will cause tremendous stress cycles day after day that is adverse for the fatigue resistance of the joint.

The stress influence line is similar to the line for the root-deck joint illustrated by Ji and Liu (2013). Thus, the truck with double and triple axles can be equivalent as a single wheel with certain cycles. The equivalent axle weight and the corresponding axle numbers derived from the monitored traffic data are used to estimate the fatigue damage of the joint.

4. Hot Spot Stress Analysis

4.1. Hot spot stress definitions

It is hard to evaluate the TD fatigue following the bridge design specification, since the specific fatigue strength detail category and the nominal stress determination method are unavailable for the joint (CEN, 2006; AASHTO, 2004). The hot spot stress method reported by the International Institute of Welding (IIW) (Hobbacher, 2009) is used to evaluate the TD fatigue.

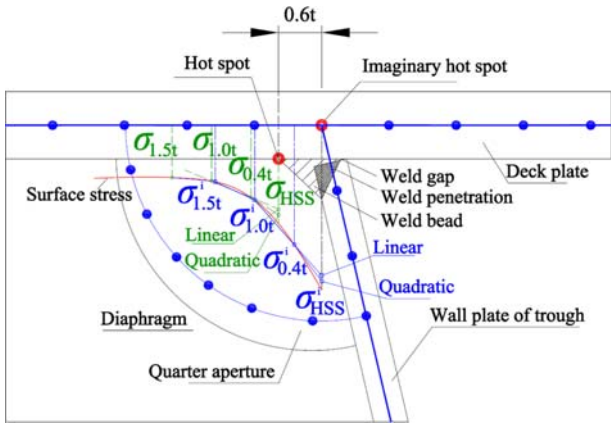

Figure 8. Definition of hot spot stress.

The basic idea of the HSS method is to create the mapping between the HSS range and the fatigue life of welded joint. The HSS consists of bending stress and membrane stress that reflect the stress raiser due to macro-geometric discontinuities. To suppress the influence of the stress singularity at the weld toe, the reference stresses $\sigma_{0.4t}$, $\sigma_{1.0t}$ and $\sigma_{1.5t}$ that represent the transverse stress σ_y located 0.4t to 1.5t from the hot spot are used to extrapolate the HSS. The linear stress extrapolation equation is shown in Eq. (1) and the quadratic one in Eq. (2), where, t represents the thickness of the deck plate.

$$\sigma_{hs}=1.67\sigma_{0.4t}-0.67\sigma_{1.0t} \quad (1)$$

$$\sigma_{hs}=2.52\sigma_{0.4t}-2.24\sigma_{0.9t}+0.72\sigma_{1.4t} \quad (2)$$

The fatigue life is determined by fatigue tests including the welding notch effects. The fatigue strength of various welded joint with the corresponding weld treatment is 90, 100, and 112 MPa (Hobbacher, 2009). The TD fatigue strength against HSS was derived by Liu (Liu *et al*., 2014a) is about 102.6 MPa, regardless of the influence of the quarter-aperture. Limited test results of the joint with aperture are available. The aperture is taken as the macro geometric discontinuity and the fatigue strength is conservatively taken as 100 MPa.

The hot spot is defined as the potential point of a welded joint where fatigue damage might occur (Hobbacher, 2009). The observed crack of the joint is close to the weld toe on the bottom surface of the deck plate. Thus, the weld toe is set as the hot spot of the joint. The shell model is used to calculate the hot spot stress. Since the weld geometry is omitted in the shell model, HSS might be underestimated. The trough to deck intersection point is defined as the imaginary hot spot in this paper, as shown in Fig. 8. The influence of the hot spot location by using the imaginary hot spot is studied. The mesh size, element shape functions and the stress extrapolation strategy is checked to determine the HSS. The joint under a single wheel load is analyzed to determine the HSS.

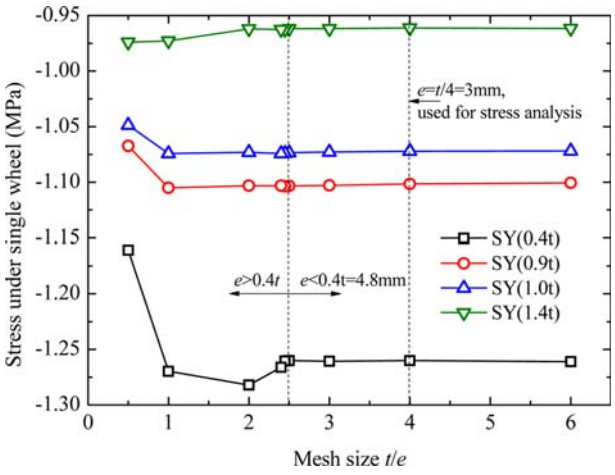

Figure 9. Influence of mesh size.

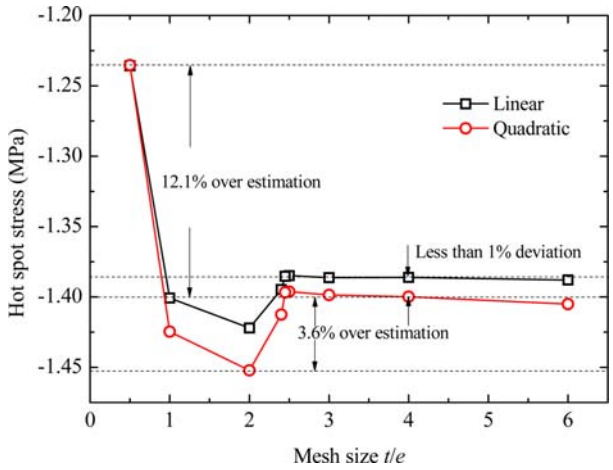

Figure 10. Influence of stress extrapolation.

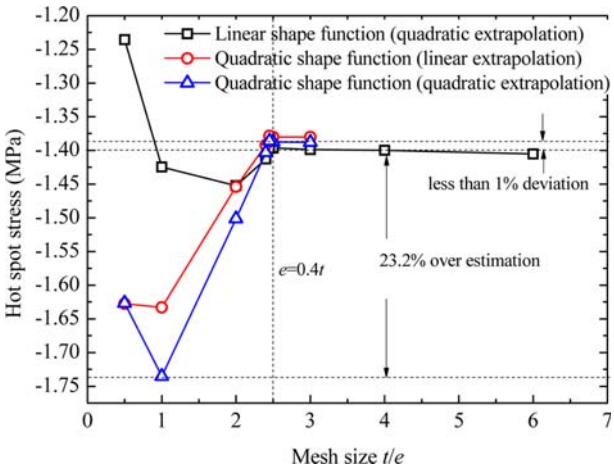

Figure 11. Influence of element shape functions.

4.2. Influence of mesh size

In order to obtain a convergent value of HSS, the reference stresses used to derive HSS are analyzed with the element length e varying from $2t$ to $t/6$. t is the deck plate thickness. Figure 9 shows the reference stresses on the bottom surface of the deck plate. The four reference stresses vary with the mesh size and tend to be constant with refined mesh. The stress results using coarse model might be underestimated. The reference stress σ_{4t} is close to the stress singularity point at the trough-deck intersection and it requires a smaller mesh size to get convergence. Given element length e is less than $t/4$, the reference stress is isolated from the stress singularity point by the intermediate element and the mesh sensitivity is suppressed. It seems that the refined shell model with e less or equal to $t/4$ is adequate to derive convergent HSS for the trough-deck welded joint.

4.3. Influence of stress extrapolation

The HSS results using linear and quadratic stress extrapolation are shown in Fig. 10. The difference between the two stress deriving methods is small with the mesh size variation since the surface stress distribution of the deck plate is relatively gentle in the region 0.4t away from the trough-deck intersection. The quadratic result is about 1% higher than the linear one while the coarse result might be 12% underestimated. It indicates that the HSS is more susceptible to the mesh size than the stress extrapolation. Although the quadratic result might be less than the linear one if the stress gradient decreases at the point that is closer to the weld toe, the quadratic result is used since the stress peak under a wheel load shows increasing stress gradient. The HSS using 1.0t mesh size results in less than 4% stress approximations. The refined model with $t/4$ is used to get a nearly constant HSS.

4.4. Influence of element shape function

The HSS results using shell181 and shell281 that represent the linear and quadratic shape functions respectively are shown in Fig. 11. Generally, the quadratic elements are efficient to give better estimation with the coarse model for the deep stress gradient. However, the quadratic element might overestimate HSS and 23% overestimation is obtained using $1.0t$ coarse mesh. Both the linear and the quadratic elements do not come to convergence until less than t/4 refined mesh is used. The stress singularity is involved by the quadratic element shape function until the intermediate element is set. It seems that the quadratic elements require extra equations to yield the same mesh density and the HSS accuracy. For the relatively gentle stress gradient, the refined model with linear elements may be preferred for the HSS analysis.

4.5. Influence of hot spot location

The distance of the weld toe and the imaginary hot spot is about $0.6t$. Figure 12 shows the influence of the hot spot approximation. The HSS that is extrapolated based on the weld toe is 10% smaller than the imaginary hot spot. The major reason for the stress difference is that the

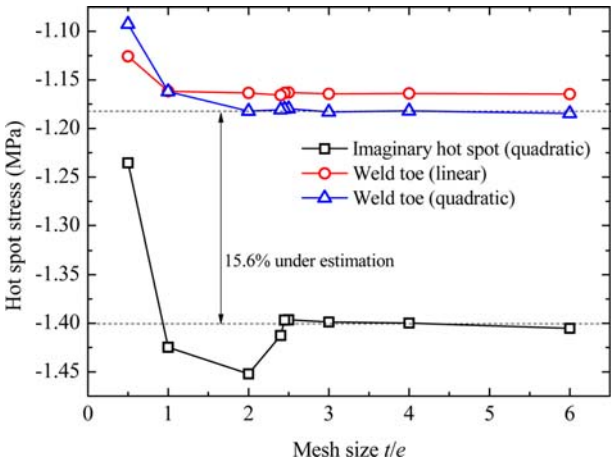

Figure 12. Influence of hot spot location.

HSS at the weld toe does not include the influence of the weld geometry and the stress might be underestimated. The HSS at the imaginary hot spot might be a little overestimated since the hot spot is extended from the weld toe. However, the imaginary hot spot gives a moderate estimation for the design application. The imaginary hot spot is used for HSS determination in this paper.

5. Fatigue Durability Evaluations

The single and double wheel loads induced HSS responses at the bottom surface of the deck plate in the trough-deck joint are illustrated in Fig. 13. The unit wheel is loaded on the shoulder lane of the deck. The critical transverse location of the wheel is determined according to Fig. 6. That is Y=200 mm for the toe-deck fatigue. The HSS responses due to the wheel transverse driving deviation are analyzed with the transverse wheel location ±100 mm and ±200 mm away from the critical path. The wheel moves over the object weld of the deck over the diaphragm. Compressive stresses are induced when the wheel is applied above the object weld and small tensile stresses are induced when the wheel is applied about 500 mm longitudinally in front of or behind the object weld. The compressive stress comes to its maximum when the wheel is located vertically on the top of the joint. Each wheel causes one major stress cycle $\Delta\sigma_1$ and one small stress cycle $\Delta\sigma_2$. The compressive stress peak contributes to the major fatigue damage and the HSS determination scheme using the shell model results in a convergent result. The corresponding fatigue strength against HSS is determined referring to those fatigue tests that simulated the increasing stress gradient towards the weld toe. The tensile HSS partially results from the decreasing stress gradient towards the weld toe since the joint is subject to out-of-plane bending of the deck. The difference in the mechanical behavior of the increasing and the decreasing stress gradient might have influence on the fatigue result. However, the fatigue strength against HSS under the tensile stress is

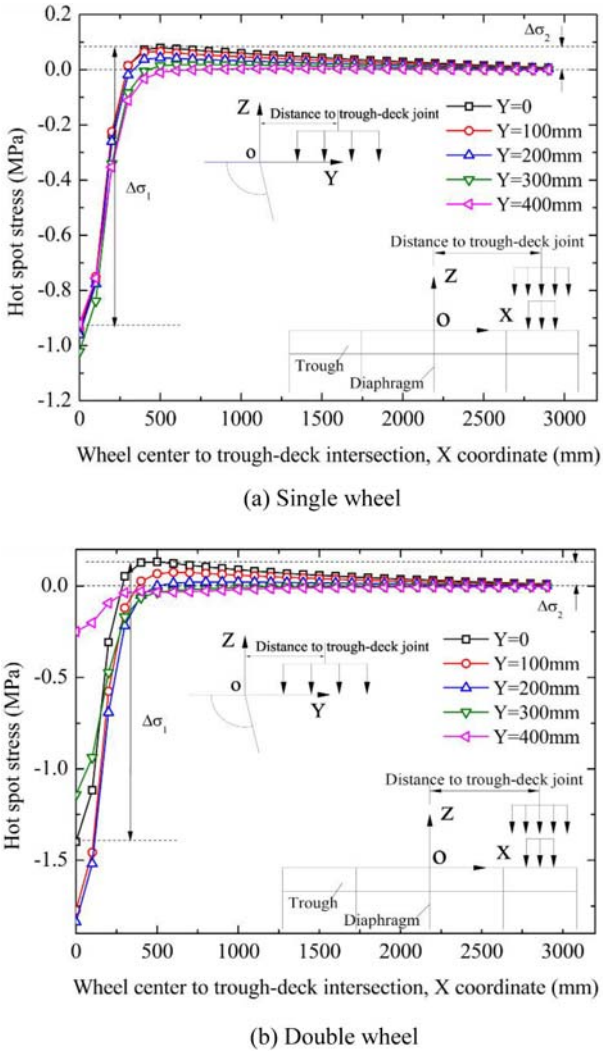

Figure 13. Hot spot stresses under wheel loads.

treated the same as the compressive one regarding the small weight of the tensile stress compared with the compressive stress and the limited fatigue tests modeling the out-of-plane bending.

The corresponding stress ranges of the stress history caused by the wheel loads are calculated by the reservoir method (CEN, 2006). The stress ranges considering the transverse driving path deviation are shown in Fig. 14. The equivalent stress ranges $\Delta\sigma_{s,d}$ representing the single and the double wheel respectively are determined considering the wheel frequency suggested by CEN (2006). The value of $\Delta\sigma_{s,d}$ is calculated by Eq. (3), where, λ_i is the wheel frequency that is 0.5 for the critical path and 0.18 for the ±100 mm path and 0.07 for the ±200 mm path. $\Delta\sigma_i$ is the stress range of the corresponding path. The constant m is 3.0. The ratio of the equivalent stress range over the critical stress range is about 0.91 for the single wheel and 0.99 for the double wheel. It indicates that the toe-deck fatigue suffers high level stress cycles even considering the transverse wheel deviation.

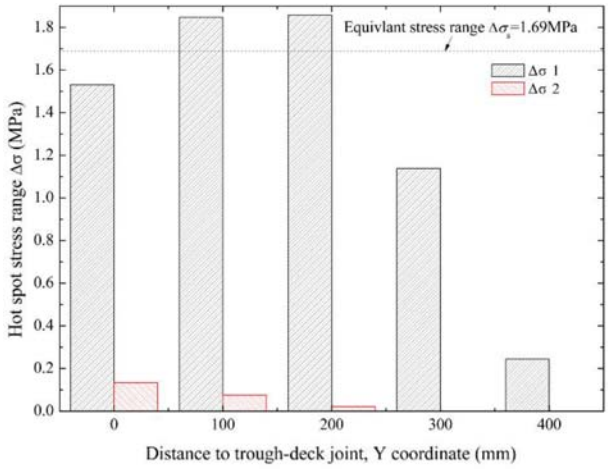

(a) Single wheel

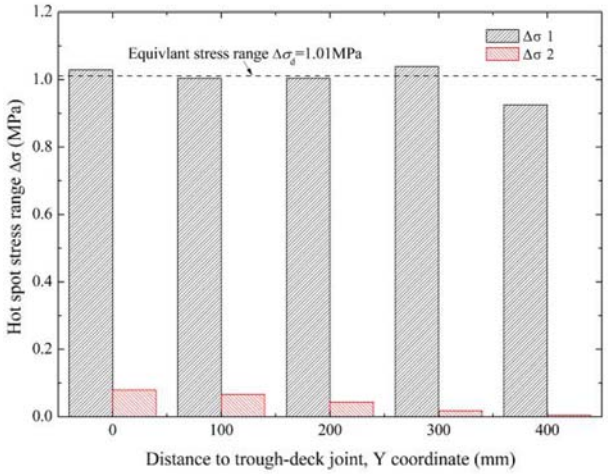

(b) Double wheel

Figure 14. Hot spot stress ranges under wheel loads.

$$\Delta\sigma_{s,d} = \left(\sum \lambda_i \times \Delta\sigma_i^m\right)^{1/m} \tag{3}$$

The fatigue damage caused by the single wheel within one year is represented by D_s and D_d for double wheels. $D_{s,d}$ is determined by Eq. (4) and the durability DU of the toe-deck fatigue is determined by Eq. (5). $WN_{s,d}$ that represents the stress cycles due to the single or the double wheels can be derived from the averaged daily truck (ADT). The wheel weight $WW_{s,d}$ can be determined either from the traffic data or the fatigue load models stipulated by the design specification. The fatigue strength against HSS $\Delta\sigma_{2\text{million}}$ for the toe-deck fatigue of the trough-deck welded joint has the mean value of 170 MPa and the mean-2s value of 100 MPa representing 2 times the standard deviation below the mean value (Liu *et al*, 2014a).

$$D_{s,d} = \frac{365 \times WN_{s,d}}{2 \times 10^6 \times \left(\frac{\Delta\sigma_{2\text{million}}}{\Delta\sigma_{s,d} \times WW_{s,d}}\right)^m} \tag{4}$$

$$DU = \frac{1}{D_s + D_d} \tag{5}$$

Given the traffic volume is 30,000/day that is about the average traffic of Jiangyin Bridge and Humen Bridge, the toe-deck fatigue is evaluated using the HSS method. The truck proportion is 0.2 and the multi-lane ratio is 0.8. ADT=30,000×0.2×0.8=4,800/day. Then, WN_s is about 1.21ADT and WN_d is about 1.69ADT that is determined using the one month toll gate collected traffic data. The wheel weight $WW_{s,d}$ is 20.8 kN for the single wheel and 50.1 kN for the double wheels. The durability results calculated using the wheel load model and the bridge design specifications are shown in Table 1. The mean-2s durability is from 2 to 12 years while the mean value is from 7 to 59 years. The fatigue cracks of Humen Bridge report after 5 years' service and the about 10 years' cracks of Jiangyin Bridge lie within the predicted fatigue durabilities. It seems that the 12 mm deck plate with 50 mm asphalt pavement over the aperture probably is not a conservative design under the heavy traffic volume. The possibility that the observed cracks in the vicinity of the trough-deck welded joint might include the toe-deck fatigue should not be eliminated.

The result by AASHTO (2004) is smaller than the wheel load model while the Japan wheel model (PWRI, 2010) gives longer prediction. The result by BS5400 (BSI, 1980) happens to be close to the wheel model in this paper. It indicates that the fatigue evaluation depends on the local traffic assumption. The 3-axles-truck model can result in a conservative design for the joint while the single and double wheel model based on the traffic monitoring system can give a more appropriate evaluation on the fatigue state of the bridge.

Table 1. Toe-deck fatigue durability

	AASHTO	This paper	BS5400	Japan
Load model	3-axles-truck	Single/double wheel	4-axles-truck	Double wheel
Wheel weight (kN)	17.5/72.5/72.5	20.8/50.1	40/40/40/40	31.8
Truck volume(/day)	4800	4800	4800	5255
Mean-2s Durability(a)	2	4	4	12
Mean durability(a)	7	21	21	59

6. Conclusions

Fatigue cracks are found in the OSD with 12 mm deck plate and 60 mm (50 mm before patching) asphalt pavement in China. The toe-deck fatigue over the aperture is evaluated using the HSS method. The following conclusions are obtained,

(1) Depending on the deformation and stress distribution of the joint under the wheel load, the aperture weakens the diaphragm's constraint to the deck plate and the trough wall. The distortion of the joint makes the exposed toe on the deck plate suffer the high stress concentration and the frequent stress cycles that might lead to the toe-deck fatigue.

(2) With the refined model, the element shape function and the stress extrapolation equation have little influence on the accuracy of HSS. The refined shell model with element length less than $t/4$ might be used to suppress the stress error. With the constant fatigue strength, the imaginary hot spot at the trough-deck intersection might be used to get a conservative HSS of the joint.

(3) According to the HSS fatigue prediction, the toe-deck crack could probably occur in the specific joint under heavy traffic flow. It seems that the hot spot fatigue theory can explain the observed fatigue example in China and the fatigue tests reported from USA. The HSS method might be used to get a conservative OSD design.

Above all, most of the bridges with the welded orthotropic steel decks serve less than 30 years in China. More fatigue cases might occur with the traffic growth. The in-site inspection of the cracks should be carried out to identify the cracks pattern and the corresponding mechanism.

Acknowledgments

The research reported herein has been carried out as part of the research projects granted by the National Natural Science Foundation of China (51108153) and Postdoctoral Science Foundation of China (2012M511188). The assistances are gratefully acknowledged. We thank the referees for their detailed comments that have helped improve this paper substantially.

References

AASHTO Inc. (2004). *LRFD bridge design specifications.* 3rd Ed., Washington, DC.

Ansys Inc. (2013). Mechanical user's guide, Canonsburg, PA.

BSI (1980). *Steel, concrete and composite bridges, BS5400: Part 10. Code of practice for fatigue*, British Standards Institution, pp. 7-8.

De Jong, F. B. P. (2004). "Overview fatigue phenomenon in orthotropic bridge decks in the Netherlands." *Proc. 2004 Orthotropic Bridge Conference*, Sacramento, California, USA, pp. 25-27.

CEN (2006). Eurocode 3: Design of steel structures. Part 2: Steel Bridges. *ENV 1993-2*, European Committee for Standardization.

Fisher, J. W. and Roy, S. (2014). *Durability of steel orthotropic bridge decks. Bridge maintenance, safety, management and life extension*. Taylor & Francis Group, London, 978-1-138-00103-9, pp. 117-130.

Hobbacher, A. (2009). *Recommendations for fatigue design of welded joints and components*. IIW doc.1823-07, Welding Research Council Bulletin 520, New York.

JRA (2002). Fatigue design guidelines for steel highway bridges, Japan Road Association, Tokyo (in Japanese).

Ji, B. H. and Liu, R. (2013). "Evaluation on root-deck fatigue of orthotropic steel bridge deck." *Journal of Constructional Steel Research*, 90, pp. 174-183.

Kolstein, M. H. (2007). *Fatigue classification of welded joints in orthotropic steel bridge decks*. Ph.D. Dissertation, T.U.Delft.

Liu, R., Ji, B. H., Wang, M. M., Chen, C., and Maeno, H. (2014a). "Numerical evaluation of toe-deck fatigue in orthotropic steel bridge deck." *Journal of Performance of Constructed Facilities,* 04014180. pp. 1-10.

Liu, R., Liu, Y. Q., Ji, B. H., Wang, M. M., and Tian, Y. (2014b). "Hot spot stress analysis on rib-deck welded joint in orthotropic steel decks." *Journal of Constructional Steel Research*, 97, pp. 1-9.

Miki, C., Tateishi, K., Okukawa, A., and Fuji, Y. (1995). "Local stress and fatigue strength of the joint between longitudinal and transverse ribs in orthotropic steel deck plate." *Journal of Japan Society of Civil Engineering*, 519(32), pp. 127-137 (in Japanese).

Miki, C. (2006). "Fatigue damage in orthotropic steel bridge decks and retrofit works." International Journal of *Steel Structures,* 6(4), pp. 255-267.

Mori, T., Shigihara, S., and Nakamura, H. (2006). "Fatigue tests on welded connections between deck plate and trough rib in steel plate deck in consideration of welded penetration." *J. of JSCE*, 62(3), pp. 570-581 (in Japanese).

Pan, P., Li, Q. W., Zhou, Y. B., Li, Y. S., and Wang, Y. Q. (2011). "Vehicle survey and local fatigue analysis of a highway bridge." *China Civil Engineering Journal*, 44(5), pp. 94-100 (in Chinese).

PWRI (2010). *Cooperative research report of fatigue durability improvement technology of orthotropic steel bridge deck.* No. 398, part 2, Public Works Research Institute, Ibaraki, pp. 44-54 (in Japanese).

Sim, H. B., Uang, C. M., and Sikorsky, C. (2009). "Effects of fabrication procedures on fatigue resistance of welded joints in steel orthotropic decks." *Journal of Bridge Engineering*, 14(5), pp. 366-373.

Wolchuk, R. (1999). "Steel orthotropic decks developments in the 1990s." *Transportation Research Record*, No. 99-0430, 1688, pp. 30-37.

Xiao, Z. G., Yamada, K., Ya, S., and Zhao, X. L. (2008). "Stress analyses and fatigue evaluation of rib-to-deck joints in steel orthotropic decks." *International Journal of Fatigue*, 30(8), pp. 1387-1397.

Yuan, H. (2011). *Optimization of rib-to-deck welds for steel orthotropic bridge decks*. Virginia Polytechnic Institute

and State University. Blacksburg, VA.

Zhou, Y. B. (2010). *Crack study and local fatigue analysis of orthotropic steel decks on bridges*. Tsinghua University, China (in Chinese).

Zhang, L. F., Ai, J., Zhang, P. F., and Yang, C. H. (2013). "Damage and cause analysis of steel box girder in long span bridges." *Chinese Journal of Highways and Automotive Applications*, 156(3), pp. 203-206 (in Chinese).